

Parametric Analysis of the Selective Laser Sintering Process

Ming-shen Martin Sun, Joseph J. Beaman, and Joel W. Barlow
The University of Texas at Austin

Abstract

Qualitative and quantitative analyses are required to develop Selective Laser Sintering into a viable Manufacturing process. A simplified mathematical model for sintering incorporating the heat transfer equation and the sintering rate equation, but using temperature independent thermal properties, is presented in this paper. A practical result is the calculation of sintering depth defined as the depth of powder where the void fraction is less than 0.1 as a function of control parameters, such as the laser power intensity, the laser scanning velocity, and the initial bed temperature. We derive the general behavior of laser sintering. A comparison of model predictions with laser sintering tests is provided.

Introduction

The previous works on the Selective Laser Sintering have been concentrated on exploring suitable sintering materials and experimentally determining the control parameters. Little theoretical research has been done beyond Frenkel's sintering model [1]. However, a better model that predict the sintering behavior correctly could save a lot of experimental work. We here propose a simplified integrated model for Selective Laser Sintering which, through the verification of true sintering experiments, proved to be a valuable basis of the more sophisticated models to be developed in the future. It can also be used in the instructive parametric analysis of the sintering behavior.

Treating the Selective Laser Sintering process as a system, the input variables are laser power and scanning rate. Output variables of this system should practically describe the quality of the sintered part. One important indication of part quality is its void fraction. Temperature acts as a intermediate state variable in this model. There are some other factors affecting the sintering process, such as the initial powder bed temperature, air flow condition, the optical, thermal and rheological properties of the powder, and the morphology of the powder. A conceptual model for selective laser sintering is thus derived as shown in Fig.1.

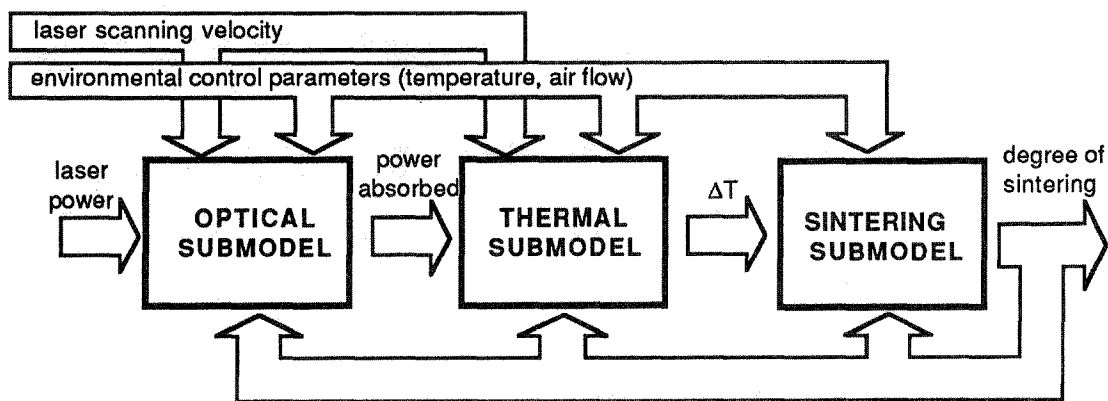


Figure 1. The Integrated Model of Selective Laser Sintering

This model is composed of three parts, the optical submodel takes the input laser power, combines the geometric effect of the powder and the optical properties of the material, and calculates the heat source function inputted to the thermal submodel. The thermal submodel applies the heat transfer equation in a heterogeneous porous material and calculates the temperature increase in the powder. The sintering submodel takes the temperature data, calculates the corresponding rheological properties, feeds these parameters into a sintering rate equation, and integrates to get the desired output, sintered density. This output is fed back into each submodel as a modulation. Theoretical details on the thermal and sintering submodels are discussed in the following section.

The sintering quality, which is defined by the density distribution within the sintering space, is primarily controlled through varying the laser parameters or environmental conditions. Laser parameters includes the laser power and laser scanning speed. The environmental condition includes the initial bed temperature and the boundary air convection. Directly relating the control parameters and the output quantity through experimental work is often very time and material consuming, and the result might not be very illustrative. This model provides a way of theoretical calculation through a series of individually provable submodels, and the integral result can be verified with a simple sintering experiment.

Model

For the reason of simplification, the optical submodel is not considered at this stage, the system with only thermal and sintering submodels is used assuming the input to the thermal submodel is known.

A. Thermal Submodel

A schematic diagram of Selective Laser Sintering process is shown in Fig.2

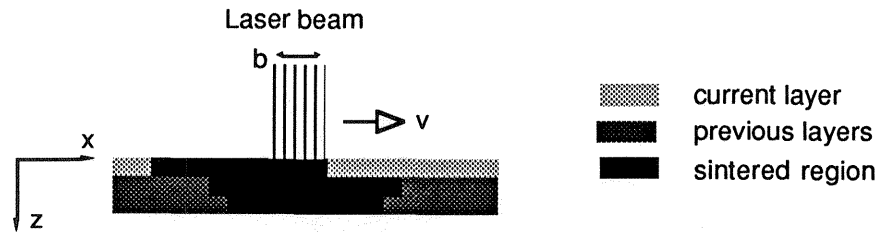


Figure 2. The Selective Laser Sintering System

The heat transfer problem in this system can be described by the partial differential equation:

$$\rho C_p \frac{\partial T}{\partial t} = \nabla \cdot (K \nabla T) + g(\underline{x}, t) \quad (1)$$

where T is the temperature increase at position \underline{x} , ρ is the apparent density, C_p is the specific heat, and K is the apparent thermal conductivity of the sintering powder at that position. The laser acts as a heat source which enters this problem either as a boundary condition (boundary heat source) or as the $g(\underline{x}, t)$ term (internal heat source). The term $g(\underline{x}, t)$ is taken as zero in this work.

Equation (1) is actually a three dimensional problem in space, and can be simplified to a two dimensional one by assuming radial symmetry. Further simplification to one dimensional is done by Festa [2] with numerical calculations. In a boundary laser heating problem, if the dimensionless parameter N , which is defined as

$$N = \frac{vb}{2\alpha} \quad (2)$$

is larger than 3, the 2-D problem can be approximated by a 1-D problem within a 5% error. In equation (2), v is the laser scanning velocity, b is the laser spot size and α is the apparent thermal diffusivity of the material. Since in most cases of the Selective Laser Sintering, the value of N is higher than 1000, it is proper to use the 1-D approximation, and the PDE becomes:

$$\rho C_p \frac{\partial T}{\partial t} = \frac{\partial}{\partial z} \left(K \frac{\partial T}{\partial z} \right) \quad (3)$$

with the boundary conditions:

$$\begin{aligned} -K \frac{\partial T(0,t)}{\partial z} = q(t) &= \begin{cases} q_0 & \text{for } 0 \leq t \leq \tau \\ 0 & \text{for } t > \tau \end{cases} \\ T(z,t) \rightarrow 0 & \quad \text{for } z \rightarrow \infty, t > 0 \end{aligned} \quad (4)$$

The properties ρ , C_p and K will vary as sintering proceeds. The change is primarily caused by the change in porosity. Yagi and Kuni [3] proposed a formula relating the effective thermal conductivity of a porous material to its volume void fraction ε :

$$K_{eff} = \beta (1-\varepsilon) \frac{K_s}{(1+\phi K_s/K_g)} \quad (5)$$

where $\beta \cong 1.0$ and $\phi = 0.02 \times 10^{2(\varepsilon - 0.3)}$ from experimental data, and K_s and K_g are the thermal conductivity of the solid material and the air respectively.

The apparent density of the powder is:

$$\rho = \rho_s(1 - \varepsilon) \quad (6)$$

and considering the mass of the air within the powder is negligible, the specific heat of the powder is equal to the specific heat of the solid material.

B. Sintering Submodel

The process of sintering includes heating up the powder, melting or softening the material (decrease its viscosity), particles coalescence due to the surface tension force, and finally cooling and solidifying. Frenkel [1] first derive a model describing the sintering behavior of two particles under a constant temperature, the model is an equation describing the neck radius growing with time. The idea behind this model is to equalize the energy change due to the surface area reduction to the energy dissipated in the viscous mass flow between particles. This model provides a qualitatively useful idea of the effect of surface tension and melt viscosity in sintering.

Using Frenkel's idea, Scherer [4,5] has developed a sophisticated model of viscous sintering of porous material by approximating the porous structure with a cylinder network structure. This approach provides an explicit relation between the change in porosity, or what he defined the changing rate of the free strain e , the surface tension σ , the viscosity η , and the current geometry :

$$\frac{\partial e}{\partial t} = -\frac{M}{\eta} \frac{(3\pi)^{1/3}}{6} \frac{2-3cx}{\sqrt[3]{x(1-cx)^2}} \quad \text{when } \rho \leq 0.94 \rho_s \quad (7)$$

$$\frac{\partial e}{\partial t} = -\frac{M}{\eta} \frac{1}{2} \left(\frac{4\pi}{3}\right)^{1/3} \left(\frac{\rho_s}{\rho} - 1\right)^{2/3} \quad \text{when } \rho > 0.94 \rho_s \quad (8)$$

where

$$M \equiv \left(\frac{\sigma}{a_0}\right) \left(\frac{3}{4\pi}\right)^{1/3} \quad (9)$$

σ is the surface tension, a_0 is the initial radius of spherical particle, $c = 8\sqrt{2}/3\pi$, and x is the geometry factor defined as the ratio of the radius of the cylinder structure to the length of the cylinder.

The void fraction can be related to the free strain and the geometry factor by:

$$\varepsilon = 1 - (1 - \varepsilon_0) \exp(-3e) \quad (10)$$

$$\varepsilon = 1 - 3\pi x^2 + 8\sqrt{2} x^3 \quad (11)$$

This model provides an useful relation between the geometry and the temperature related rheological properties.

As the main effect of temperature is to change the viscosity, the Arrhenius form of viscosity should be used:

$$\eta = A \exp\left(\frac{\Delta E}{RT}\right) \quad (12)$$

where the coefficient A and the activation energy ΔE can be determined from the standard viscosity tests on the polymer melt.

Computer Simulation

The models described above have been implemented numerically into a computer program. This program incorporates a finite difference equation, which solves the heat conduction problem with the thermal properties modulated by the void fraction, a sintering rate equation, which use the rheological properties modulated by the temperature to integrate the resulting void fraction .

The structure of the program is shown in Fig. 3.

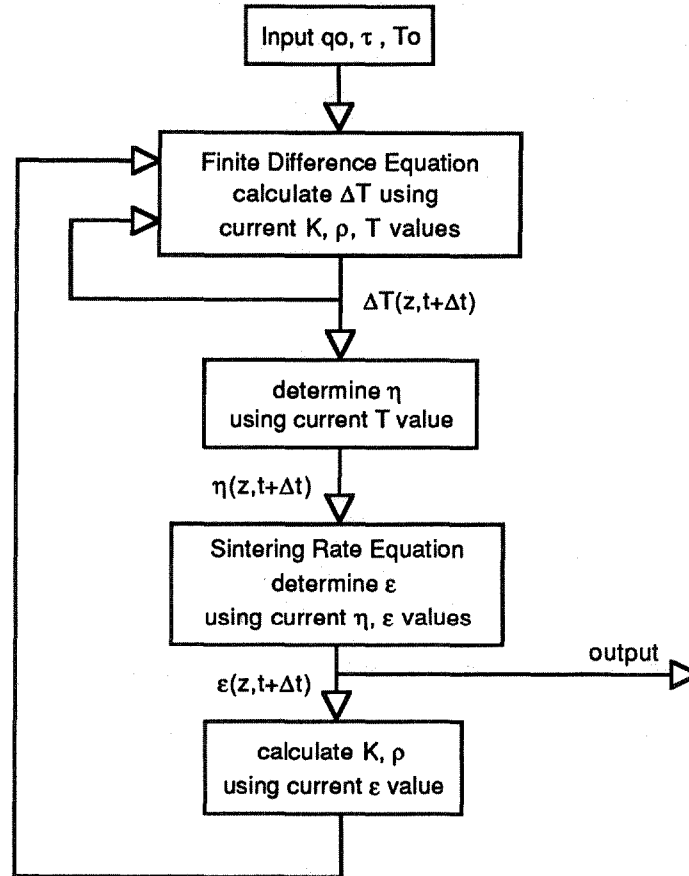


Figure 3. The Structure of the Simulation Program

Properties of the material have been determined through various experiments. These values are inputted to the program, and with a selected laser power intensity q_0 , laser exposure time τ , and initial bed temperature T_0 , the program can calculate the temperature increase and void fraction in any position at any time. A typical calculation result is shown in Fig.4.

From the result (Fig.4), an iso-void-fraction curve (Fig.5) plot in the t - z plane can be constructed. This plot shows that the position of the iso-void-fraction tends to settle to a steady state value which is determined by the control parameters q_0 , τ and T_0 . If we define a sintering depth d as the steady state depth position above which the void fraction are smaller than 0.1 (a typical void fraction of a sintered material), and by running the computer model with varying q_0 , τ and T_0 value, we can analyze the basic sintering behavior. Some of the computer simulation results are shown in Fig.6-8.

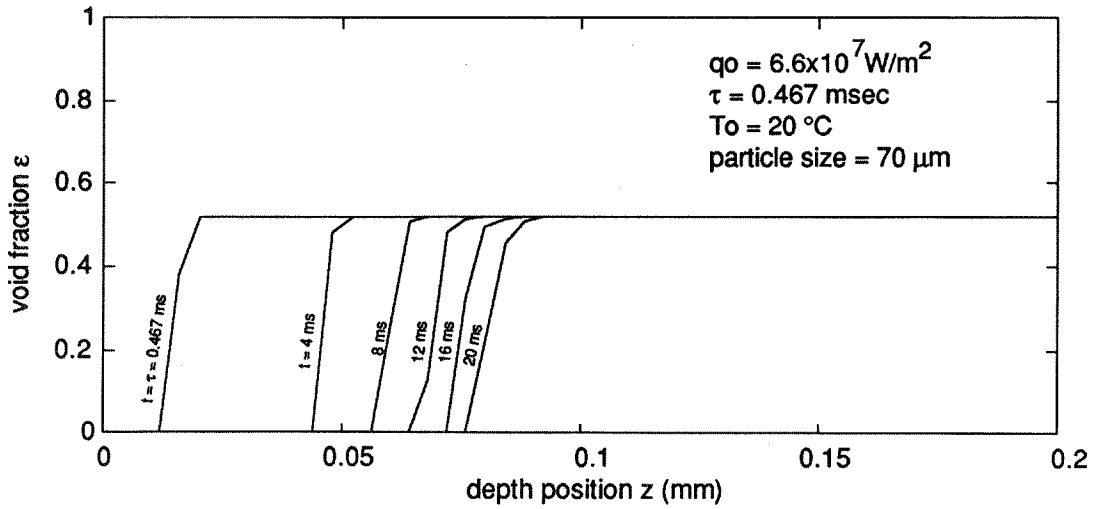
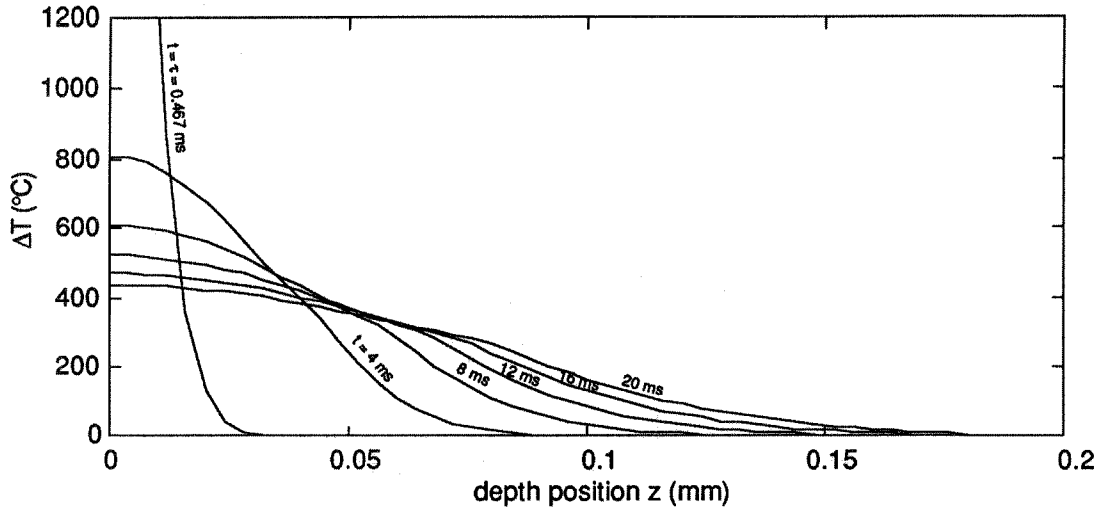


Figure 4. A Typical Computer Model Calculation Result: Using material properties of ABS

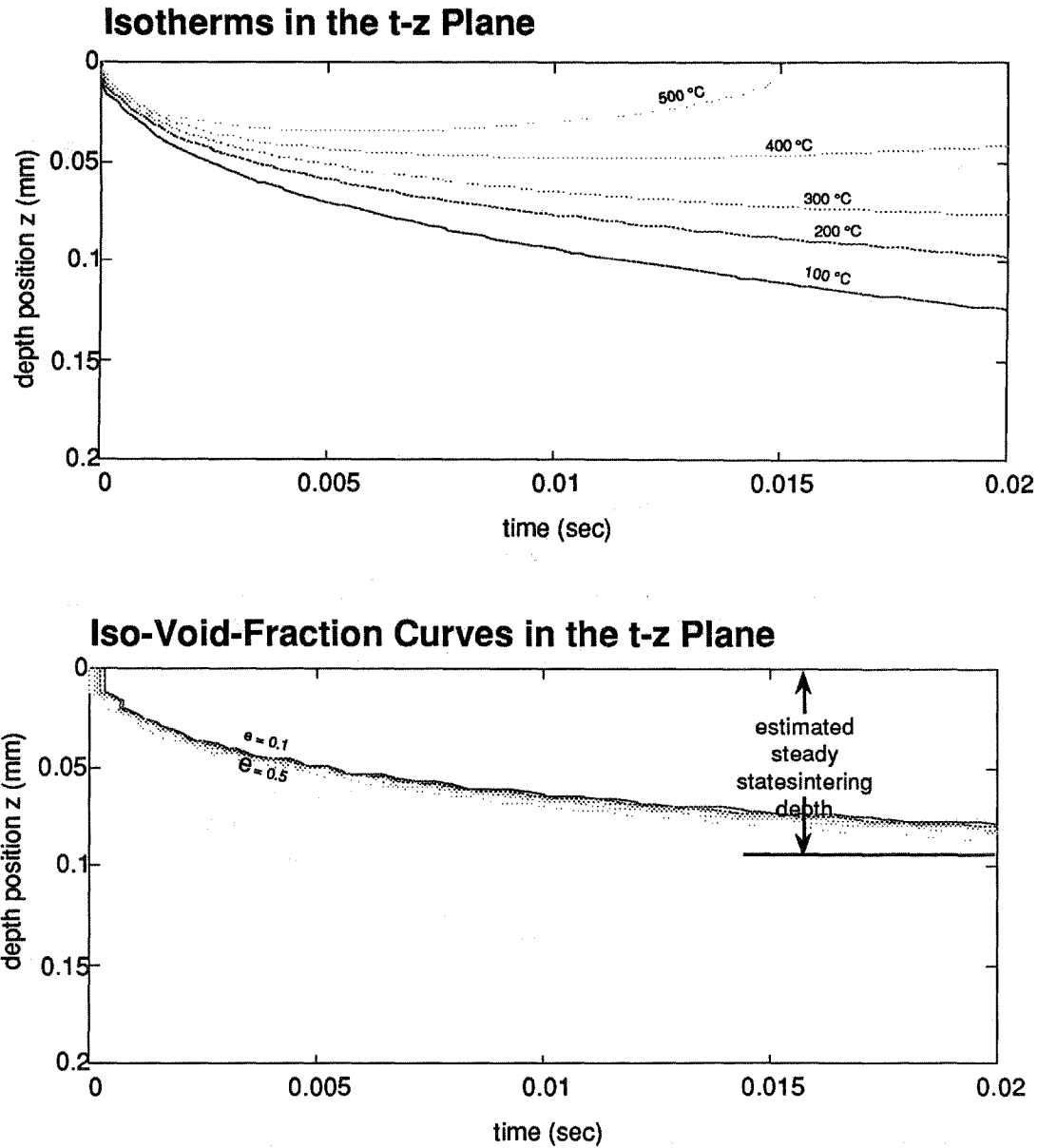


Figure 5. The Isotherms and Iso-Void-Fraction Curves in the t-z Plane

Selective Laser Sintering Experiments

In order to verify the simulation results, experiments run on a actual Selective Laser Sintering machine are conducted. These experiments are done by laser scanning a 1"x1" square pattern on a smooth powder surface using different laser power and scanning speed at different bed temperature. Power intensity and exposure time can be calculated from the power, the scanning rate, and the spot size. After cooling, the thickness of the sintered pattern is measured directly under the microscope or indirectly by weighing the sintered pattern and dividing by the pattern area and the sintered density.

Some of the experimental values for the ABS powder are shown in Fig.6-8. These results show the same qualitative behavior as the computer model. Differences between the simulation and experiment are caused by the inaccuracy in measuring the laser parameters, the difficulty in measuring the sintered depth, and by assumptions of temperature independent specific heats and thermal conductivities.

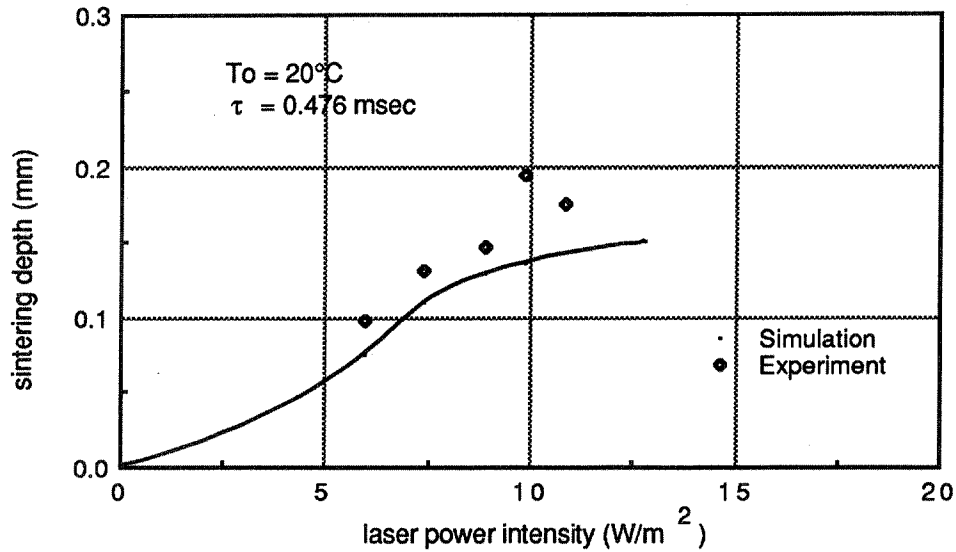


Figure 6. Laser Sintering Experiment I: Varying Laser Power

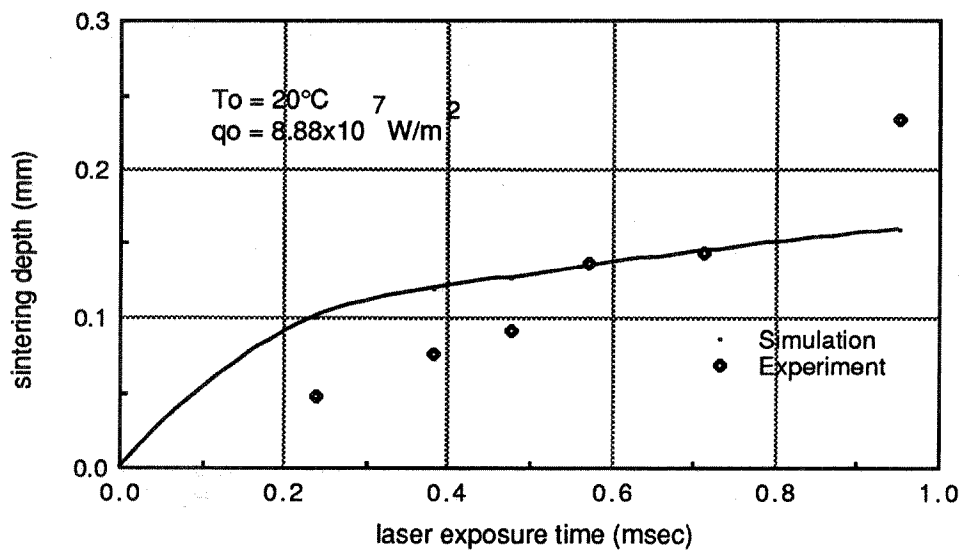


Figure 7. Laser Sintering Experiment II: Varying Laser Scanning Velocity

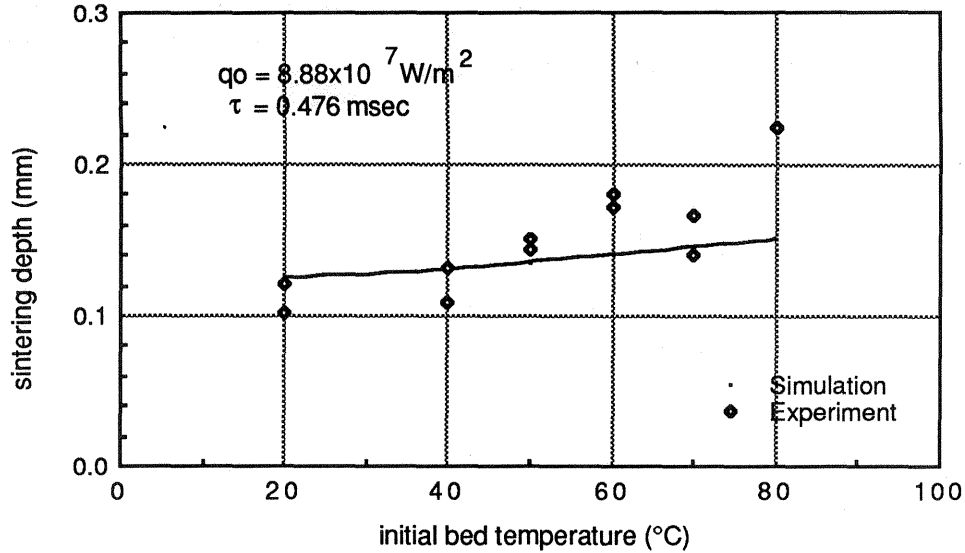


Figure 8. Laser Sintering Experiment II: Varying Initial Temperature

Conclusion

An integrated model of Selective Laser Sintering is presented in this paper. By implementing this model into a computer simulation program, parametric analysis can be done to guide the experimental work. This can be used to optimize the process parameters or to find out the proper sintering materials. The sintering model predicts very well the sintering behavior observed. The prediction can be improved more by finding the accurate parameter values.

Future work to improve this model will be to include the optical submodel to account for the laser reflection and penetration effect, to use better numerical integration algorithms, and to increase the discretization to get a better accuracy. Also by conducting separate experiments to verify each submodel, a more powerful version of this model is foreseen.

References

1. Frenkel, J., J. Phys. (USSR) 9:385, 1945
2. Festa, R., Manca, O. and Naso, V., "A Comparison Between Models of Thermal Field in Laser and Electron Beam Surface Processing", Int. J. Heat Mass Trans. Vol.31, No.1, pp99-106, 1988
3. Yagi, S. and Kuni, D., "Studies on Effective Thermal Conductivities in Packed Beds", J. AIChE. Vol.3, No.3, pp373-381, 1989
4. Scherer, G., "Sintering of Low-Density Glasses: I, Theory", J. Am. Cer. Soc. Vol.60, No.5-6, pp236-239, 1977
5. Scherer, G., "Viscous Sintering under a Uniaxial Load", Comm. Am. Cer. Soc. Vol.69, No.9, pp206-207, 1986